PHYSICAL REVIEW B VOLUME 47, NUMBER 24 15 JUNE 1993-II

Growth of germanium films on Si(001) substrates

Christopher Roland
Department of Physics, North Carolina State University, Raleigh, North Carolina 27694-7907

George H. Gilmer
AT&T Bell Laboratories, 600 Mountain Avenue, Murray Hill, New Jersey 07974
(Received 4 November 1992)

We have studied the growth of Ge layers on the Si(001) surface using molecular-dynamics techniques. In order to relieve the strain resulting from the lattice mismatch between Ge and Si atoms, Ge deposited on the Si(001) surface tends to form islands. This tendency to form three-dimensional structures was studied by monitoring the chemical potential of relaxed Ge films on top of the Si(001) surface. We find that layer-by-layer growth is favored for the first three layers of Ge deposited. To study the diffusion of Ge adatoms on $Ge_nSi(001)$ films, we have mapped out the potential-energy surfaces on such films with (2×1) and $(2\times N)$ reconstructions. For surfaces subject to (2×1) reconstructions, the motion is anisotropic, with the fast-diffusion direction being along the dimer rows. In the case of a surface with $(2\times N)$ reconstructions, fast diffusion is still along the dimer rows. However, we find additional potential-energy barriers where the missing dimers are located, which effectively confines the motion of adatoms. Finally, we have studied the initial stages of island formation by directly simulating the epitaxial growth of Ge layers on the Si(001) surface.

I. INTRODUCTION

In the last several years, the growth of Ge layers on top of the Si(001) surface has been the subject of intense study. Much of the driving force behind this effort has been the desire to fabricate Si-Ge heterojunction superlattices which would form the basis of optoelectronic devices.[1] However, despite the considerable progress achieved,[2] there is much that remains to be understood. Recently, important questions have been raised regarding domain structures,[3] alloy ordering and surface segregation,[4-7] and the formation of islands.[8-11]

To address some of these issues, we have carried out an extensive molecular-dynamics study of the growth of Ge layers on Si(001). Thin-film growth during molecular-beam epitaxy (MBE) is a highly nonequilibrium process, in which the growth kinetics may play an important role. In the case of Ge on Si, this process is further complicated by the effects of strain coming from the lattice mismatch between the Si and Ge atoms.

During MBE growth on low-index surfaces, atoms from the vapor condense onto a substrate. If the temperature is sufficiently high, the adatoms make their way at random across the surface, until they encounter either a two-dimensional island or other adatoms. There, the adatoms may be incorporated into the crystal via the growth or nucleation of islands. Such two-dimensional islands continue to grow, eventually merging to form a continuous layer. In the case of Ge on Si(001), the layers formed are under strain, whose associated energy increases as the film thickens. Eventually, three-dimensional clusters or islands, in which the strain is relieved by misfit dislocations, begin to form. We have investigated such Stranski-Krastanov growth by studying the energy and chemical potential of $Ge_nSi(001)$ film structures (here n denotes the number of Ge layers deposited). In agreement with experimental[8,10-12] and recent theoretical studies,[13,14] we shall show that up to three layers of Ge may be deposited on Si(001) before there is any driving force for clustering. In addition, the second and third layers are subject to a $(2\times N)$, rather than the more usual (2×1) reconstruction.

Central to any discussion of the growth kinetics of thin films is the role played by surface diffusion. To study Ge diffusion on $Ge_nSi(001)$, we have mapped out the potential-energy surfaces seen by Ge adatoms over the Si(001) and $Ge_nSi(001)$ surfaces. Surfaces with both (2×1) and $(2\times N)$ reconstructions were considered. From such energy maps, we obtain microscopic information about the binding sites, as well as the activation energies for diffusive jumps. We will show that, in many respects, the diffusion of Ge on a surface with (2×1) reconstruction resembles that of Si on Si(001).[16-18] Diffusion is predicted to be anisotropic, with fast diffusion taking place in the channel separating dimer rows. In the case of Ge on Si(001), the fast-diffusion direction has an activation energy of 0.64 eV. However, on a Si substrate covered with a monolayer of Ge, the activation energies for Ge motion in the "fast" direction were found to be considerably less (about 0.40 eV) than that of Si (about 0.67 eV), so that much faster diffusion is expected. On a surface terminated with $(2\times N)$ reconstructions, diffusive motion is still anisotropic, with fast diffusion taking place along the dimer rows. However, additional diffusion barriers found near the missing dimers will act to confine the adatom motion. This should lead to an enhanced nucleation rate of two-dimensional islands, and therefore a much rougher surface.

These results are in good agreement with recent scanning tunneling microscopy (STM) studies by Lagally and co-workers,[19] who estimated the activation energy for Ge diffusion on Si(001) to be 0.59±0.1 eV, and 0.45 eV for Ge diffusion on Ge_nSi(001).

We have also simulated the growth of Ge layers directly with molecular-dynamics methods. In agreement with experiments, the first Ge monolayer grows in a layer-by-layer fashion. We observe the formation of highly elongated islands or dimer strings, similar to those observed in the growth of Si layers.[20] We observe some evidence of three-dimensional clustering for Ge deposited on three- and six-layer Ge films, although the fast deposition rates needed for molecular-dynamics simulations afford little time for the material to aggregate.

A brief outline of the paper is as follows. In Sec. II, we discuss the energetics of Ge_nSi(001) film structures. In Sec. III, we present results on the diffusion of Ge adatoms over Ge_nSi(001), where the uppermost surface is terminated with both the (2×1) or $(2\times N)$ reconstructions. Section IV reports on some direct simulations of Ge MBE, with an emphasis on the initial stages of clustering. Finally, Sec. V is reserved for a summary.

II. STRUCTURE OF GERMANIUM FILMS ON Si(001)

Before studying growth, which is a far from equilibrium situation, it is important to understand the equilibrium structures of the system. On the basis of equilibrium thermodynamics, there are three basic modes for heteroepitaxial growth: these are Frank–van der Merwe,[21] Volmer-Weber,[22] and Stranski-Krastanov.[23] These are illustrated in Fig. 1. Loosely speaking, these may be described as layer-by-layer growth, island growth, and layer-by-layer plus island growth. The growth mode that the system adopts depends crucially on the interfacial free energy, and the lattice mismatch between the atoms in the film and the substrate. For lattice-matched systems, the growth mode selected is either layer by layer or Volmer-Weber, depending upon whether the film wets the substrate or not. For systems with low interfacial energy and a large lattice mismatch, the initial growth takes place in a layer-by-layer fashion. However, as the film thickness increases, the strain energy continues to build up, and the system can eventually lower its free energy by forming three-dimensional islands in which the strain is relieved by misfit dislocations.[24–26] Stranski-Krastanov growth is the result.

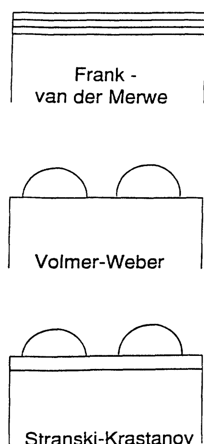

FIG. 1. A schematic diagram illustrating the three thin-film growth modes, based on equilibrium thermodynamics.

Ge atoms are about 4% larger than Si atoms, so that Si-Ge systems are characterized by a considerable lattice mismatch. Experimental studies[8,10–12] show that Ge on Si(001) forms about three to six rough layers before switching to the three-dimensional island growth mode, so that the system displays classic Stranski-Krastanov growth behavior. Recent studies, however, show that the growth may be more complex: Mo *et al.*[9,10] have observed the formation of coherent "hutlike" structures on Ge_3Si(001), and have suggested that these metastable structures provide a kinetic pathway for three-dimensional island growth; while Eaglesham and Cerullo[8] have observed the growth of dislocation-free Ge islands on Si(001).

To study the structure of Ge films on Si(001), we have measured the energy and chemical potential of relaxed Ge layers on Si(001). In agreement with experiments, and recent theoretical work by Tersoff utilizing a Keating model,[13,14] we find that up to three continuous layers of Ge may be deposited on Si(001) before three-dimensional islanding begins. On the second and third Ge layers, the $(2\times N)$ "missing dimer" reconstruction, rather than the more usual (2×1) reconstruction, is favored (see Fig. 2). Such $(2\times N)$ reconstructions, with $N\approx8$, have been observed in recent STM studies of Ge films.[10] The $(2\times N)$ reconstruction can be thought of as another strain relief mechanism: While simply removing a dimer from the surface does relieve strain, by giving the Ge external room into which to expand, this removal also creates extra dangling bonds. As proposed by Pandey,[27] these dangling bonds may be relieved by a rebonding of the second-layer atoms, at the expense of creating local tensile stress. For Ge films on Si(001), this tensile stress almost cancels the compressive stress of the film, as well as the anisotropic stress coming from the (2×1) dimer reconstruction of the surface, so that the formation of $(2\times N)$ reconstructions is favored.

We now give some details of our calculations. We constructed crystal structures terminated with a properly dimerized surface. The silicon substrates consisted of 8×10 atoms per atomic layer, and a height of at least 24 atomic layers. The atoms were then slowly relaxed using dissipative forces, with standard molecular-dynamics

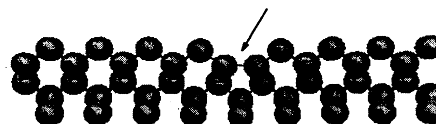

FIG. 2. The structure of the Ge_nSi(001) $(2\times N)$ surface projected onto the [011] plane. The arrow marks the position of the missing dimer. Note that the second-layer atoms have shifted to form a bond.

techniques.[28] In this way, the structures were able to find their minimum-energy configurations. Periodic-boundary conditions were used in the horizontal directions. The energies of the relaxed film structures were then measured.

The Si atoms in the film structures were modeled with a Stillinger-Weber (SW) potential.[29] This empirical potential is short ranged, and consists of two terms: a pair potential term, which combines the effects of a repulsive core with an attractive tail, and a three-body term, which favors the diamond structure of bulk silicon. Because Ge, like Si, is a group-IV element, it too was modeled with the SW potential modified in two important ways. To account for the larger Ge radius, we set the parameter $\sigma_{\rm Ge}=1.04\sigma_{\rm S}$. In addition, to account for the lower melting point of crystalline Ge, the well depth of the pair potential was scaled accordingly: $\varepsilon_{\rm Ge}=(T_M({\rm Ge})/T_M({\rm Si}))\varepsilon_{\rm Si}\approx 0.74\varepsilon_{\rm Si}$, where T_M is the melting temperature of the material (under standard conditions). Also, for the Si-Ge interaction, the SW potential was used, with parameters $\varepsilon_{\text{Si-Ge}}=0.86\varepsilon_{\rm Si}$ and $\varepsilon_{\text{Si-Ge}}=1.02\sigma_{\rm Si}$.

It must be emphasized that the use of empirical potentials to model both Si and Ge is an approximation. However, for our present study, we feel that this does not represent a serious limitation. It has been shown that the SW model successfully predicts some of the bulk properties of Si, as well as the dimerization of its (001) surface.[30] While its use in modeling Ge is more uncontrolled, the aim of this study is to predict trends and qualitative features, rather than provide definitive numerical estimates of film and activation energies. Indeed, we shall show that many of the phenomena predicted by the model are in good agreement with experiment observations.

Most of the important thermodynamic properties of the Ge_nSi(001) films at low temperatures[31] can be deduced from a knowledge of the film energies (E) measured for relaxed configurations at $T=0$. To illustrate the approach to bulk thermodynamics, we have plotted $(E\text{-}N_f\mu_B)/N_0$ as a function of the normalized number of atoms in the film, as shown in Fig. 3. Here N_f is the number of atoms in the film and N_0 the number of atoms in a completed substrate layer, so that $n=N_f/N_0$ represents the number of Ge layers in the film. The chemical potential μ_B, for bulk unstrained Ge crystals at 0 K, is just the energy per atom. We not only studied the film energies of completed Ge layers, but also looked at partially filled layers at coverages of 0.2, 0.4, 0.6, 0.8, and 0.9. The films with coverages 0.8 and 0.9 corresponded to films with (2×5) and (2×10) reconstructions, with properly rebonded second-layer atoms.[32] The films at coverages 0.2, 0.4, and 0.6 were constructed by removing rows of dimers from a (2×1) surface, and then allowing the second-layer atoms to rebound, where possible, to form proper Ge(001) steps.[33] The values for these partially filled layers are not unique, since different atomic arrangements can have identical coverages.

Figure 3(a) shows that, except at a coverage of 0.2, the quantity $(E\text{-}N_f\mu_B)$ decreases as the first monolayer fills in, indicating that the Ge atoms in the GeSi(001) film structure have a lower potential energy than bulk Ge. This is not surprising, since the Ge-Si bond is stronger than the Ge-Ge bond. The initial rise at a coverage of 0.2, and at subsequent values of 0.6 and 0.8, is due to a lack of complete rebonding at the edges of islands. As the second monolayer is filled in, the deepest minimum occurs for a completed film terminated with a (2×5) reconstruction—its energy is both less than that of a two-layer film terminated with a (2×1) reconstruction and that of the single monolayer. This occurs because the "missing dimer" reconstruction more than compensates for the strain energy of the film due to the lattice misfit. Similar behavior is observed for the third monolayer. The energy minimum for the Ge_3Si(001) (2×5) surface is, however, only a tiny bit lower than that of the two-layer film. For thicker Ge layers, the local minima also correspond to the (2×5) reconstructed films, but now the values of $(E\text{-}N_f\mu_B)$ are increasing, showing that layers four and above have higher energies than bulk Ge.

The behavior of the Ge_nSi(001) films is due to the combined effect of the reduced cohesive energy of Ge and strain. To illustrate this, we have repeated our calculations, but this time changing only one variable at a time. Figure 3(b) shows the effect of increasing the radius only. Again, for the first monolayer, the minimum energy is less than that of the bulk material. This is also true for the two-layer film with the (2×5) reconstruction. For thicker films, the energy values increase, showing that material added after two layers has a higher energy than the bulk. The effects of a softer potential are shown in Fig. 3(c). Now the minimum energy values occur for completed layers. This is not surprising, because now there is no misfit strain, and therefore no driving force which favors the (2×5) reconstruction. Note that the values of the energy minima are always decreasing, albeit at very small amounts, so that the energy of each additional layer is always less than that of bulk Ge.

The film behavior may be inferred from a knowledge of the chemical potential of the system. Since $\mu=\partial E/\partial N$, the tangent to the $(E\text{-}N_f\mu_B)$ curve is $\mu\text{-}\mu_B$. As material is deposited, the chemical potential of the equilibrium film changes. However, the change is not such that all the local potential-energy minima of the film are accessed. Rather, the equilibrium film reverts to an inhomogeneous structure consisting of a linear combination of states as determined by the common tangent construction, familiar from other thermodynamic systems. In systems such as the ones shown in Fig. 3 the energy minima correspond to discrete states, and there is no smooth curve joining the states. The chemical potential for a particular thickness is determined by the energy minima at thicknesses below and above the thickness in question. The slope of the chord connecting the states gives the chemical potential for a two-phase equilibrium between these states. The chord connecting states with the lowest slope gives the ground-state chemical potential.[26]

Plots of $\mu\text{-}\mu_B$ for Ge films are also shown in Fig. 3. For N_f less than one monolayer, the structure formed consists of an inhomogeneous mixture of the bare substrate and islands of single-monolayer height. The state of lowest chemical potential is given by the line from the origin to the minimum at $N_f/N_0=1$. Similarly, μ may

be obtained for thicker films. For Ge films, Fig. 3 shows that $\mu < \mu_B$ for films up to three monolayers, with the third monolayer being terminated with the (2×5) reconstruction. For more than three layers, the chemical potential of the film is greater than that of the bulk material, so that large clusters of "bulk" Ge are stable. That the tendency to cluster is almost entirely due to the strain between the Ge film and the Si(001) substrate is easily shown. A plot of the chemical potential for a film with larger radius but equal bond energy shows that clustering can occur after just two monolayers, terminated with the $(2\times N)$ reconstruction, are deposited [Fig. 3(b)]. On the other hand, for a film having a softer potential and no lattice mismatch, there is no strain increase with thickness

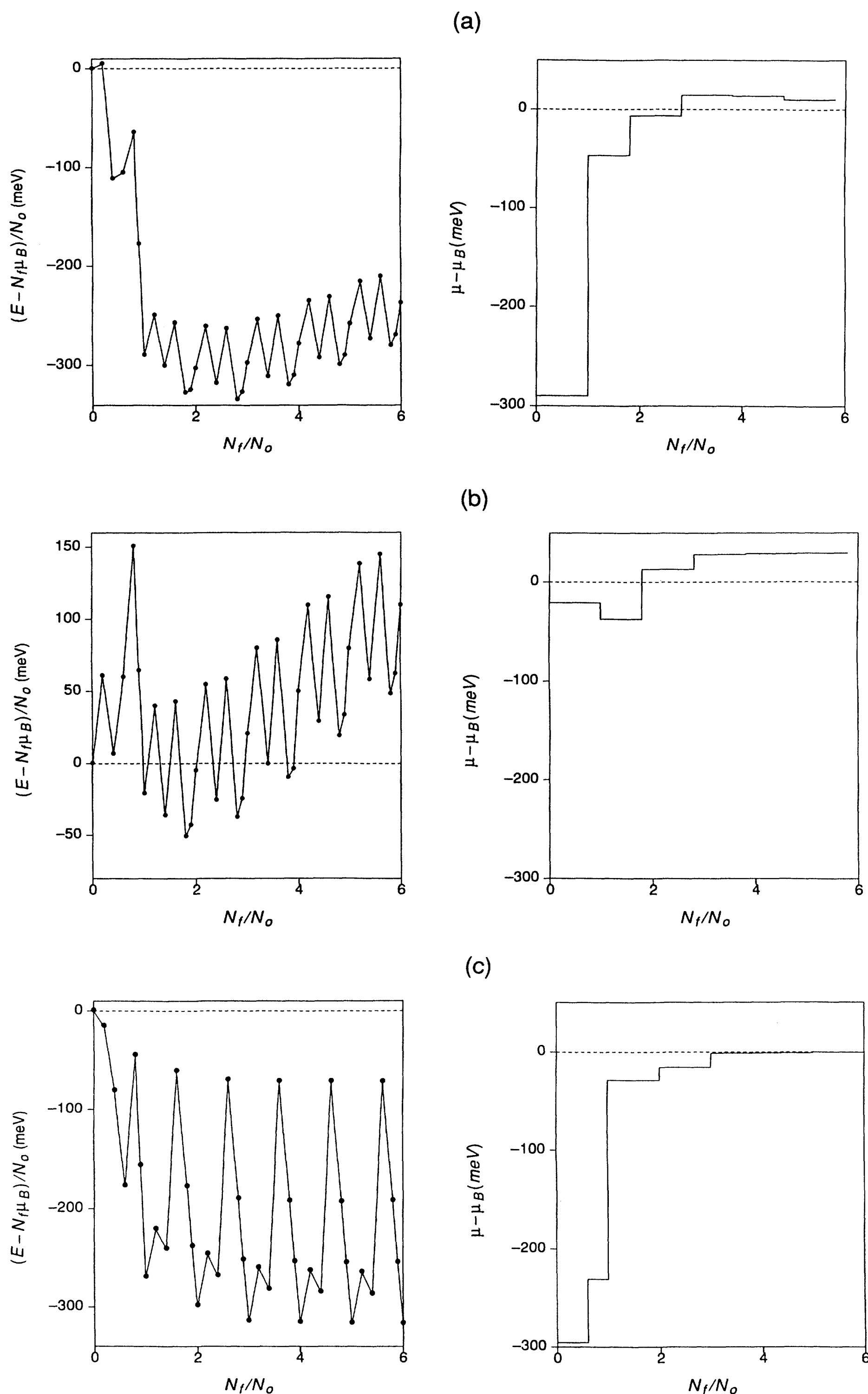

FIG. 3. The film energy per unit surface area relative to that of a bulk crystal, as well as the chemical potential differences for $Ge_nSi(001)$ films. (a) Ge films, (b) films having a larger radius only, and (c) films with a softer potential only. Here, N_f is the number of atoms in the film, and N_0 the number of atoms per substrate layer. Values corresponding to film coverage of $\frac{8}{10}$ and $\frac{9}{10}$ of a monolayer are results obtained for surfaces with (2×5) and (2×10) reconstructions.

[Fig. 3(c)]. In this case $\mu < \mu_B$ for all thicknesses, so that growth is always layer by layer.

In summary, we expect Ge on Si(001) to follow a Stranski-Krastanov growth mode, with three completed layers forming before clustering begins. The upper layer prefers to be terminated with a $(2\times N)$ "missing dimer" reconstruction. The strain resulting from the lattice mismatch between Si and Ge atoms provides the driving force for this behavior.

III. DIFFUSION OF GERMANIUM ON Ge_n Si(001) SURFACES

To study diffusion, we have mapped out the potential-energy surfaces as seen by Ge adatoms as they move over the Si(001) and Ge_3Si(001) surfaces. We studied surfaces having both (2×1) and (2×5) reconstructions. The minima on these potential-energy surfaces identify possible binding sites, while the saddle-point energies give the activation energy for diffusion hops. The most probable motion of the adatoms can then be readily identified: we shall assume that the most likely path taken is one that involves crossing the lowest possible energy barriers. Roughly speaking, the energy surface simply reflects the underlying geometry. Binding will be strong in locations where the adatom can form bonds with a number of surface atoms, preferably without distortions, and thereby reduce the number of dangling bonds. It will be weak where this is not possible. Similarly, favored pathways for adatom motion are those in which the adatoms can stay close to the substrate.

The energy surface $E(x,y)$, as a function of adatom position (x,y), was mapped out as follows. First, a flat surface having the desired reconstruction was created by placing the atoms in the appropriate positions. The system consisted of 8×10 atoms per substrate layer and a height of ten atomic layers. This atomic system was then slowly relaxed to its minimum-energy position, using weak dissipative forces, with standard molecular-dynamics methods. Periodic-boundary conditions were used in the horizontal directions. As previously discussed, the Si atoms were modeled using a Stillinger-Weber potential; the Ge with a Stillinger-Weber potential that was modified in such a way as to account for its larger atomic radius and weaker cohesive energy.

Once a relaxed configuration was obtained, an adatom was placed at some appropriate height over the surface. The system was then allowed to relax again, keeping the position of the adatom static, but allowing the other atoms to relax. The energy difference between such a system and a relaxed system with the adatom at infinity was then measured. The height of the adatom was then changed, and the process repeated. In this way, the energy at position (x,y) as a function of the height above the surface was obtained. The minimum of this function, obtained via a quadratic fit, was taken to be the value of $E(x,y)$. The process was then repeated at different grid positions, until the entire surface was mapped out. The spacing between gridpoints was chosen to be 0.24 Å. The uncertainty in the measured values of $E(x,y)$ is estimated to be less than 4%.

A. Ge diffusion on a Si(001) surface

Before presenting results on Ge diffusion over the Si(001) surface, we briefly review the diffusion of Si over the Si(001) surface.[15–18] The potential-energy map for Si over the Si(001) surface is very similar to that of Ge over the Si(001) surface, shown in Fig. 4. The chief minima on this surface, and others like it, are marked as subscripted M's. For SW Si, the global minimum lies at the "long-bridge" site (marked M_1), which is located in the channel separating dimer rows. The binding at this site is about 3.00 eV. This is a sizable fraction of 4.33 eV—which is the binding energy of bulk Si. Other local minima lie between and on top of dimers: at M_2, the binding is 2.77 eV; at M_3, it is 2.66 eV, and, at M_4, 2.60 eV. Of these, only sites M_1 and M_4 correspond to the crystal-growth sites for the new layer.

Diffusion of Si on Si(001) was found to be anisotropic, with fast diffusion taking place along dimer rows. The activation energy for such motion is, however, dependent on the path taken. If diffusion takes place in the channel separating dimer rows, the activation energy for such hops is about 0.67 eV. In our discussion, sites marked with asterisks mark corresponding sites in a neighboring

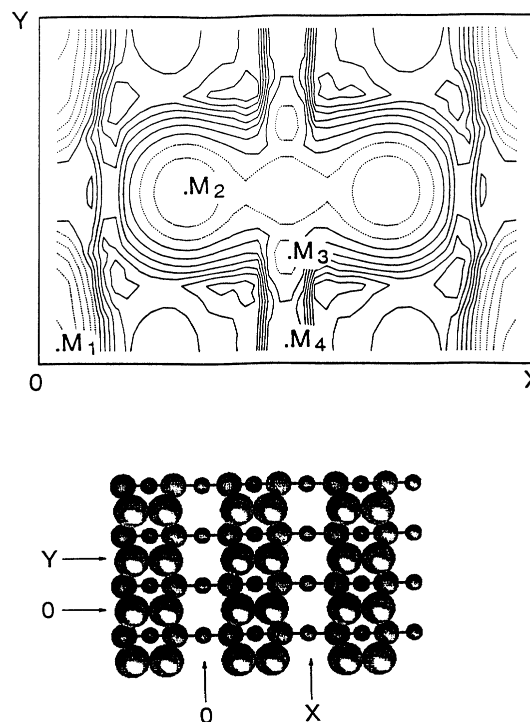

FIG. 4. The contour plot of the potential-energy surface $E(x,y)$ for a Ge adatom over the Si(001) surface, as well as the atomic positions of the Si(001) surface. The dotted contour lines in this (and all other such figures) correspond to values for which $E(x,y) < 0.50$ eV; solid contour lines indicate values $E(x,y) > 0.5$ eV. The zero point of this (and all other such figures) corresponds to the value of the global minimum M_1 on the surface. This is -3.05 eV in this case. The subscripted M's indicate the approximate positions of the local minima on the surface.

cell. If the diffusion takes place on top of the dimers, i.e., M_2 to M_4 to M_2^*, then the activation energy is a considerably lower 0.24 eV. Within the context of the SW model, we do not expect that an adatom will move along this path for very long, since the barriers for hops to M_1 are low. For motion across dimer rows, the activation energy to hop from M_1 to M_2 is about 0.76 eV, and 0.54 eV for the reverse jump. Hence the motion of Si adatoms on Si(001) is expected to take place chiefly in the channel separating dimer rows. Adatoms which initially land on top of dimer rows eventually find the global minima at M_1 and move along the dimer rows. A molecular-dynamics simulation of adatom diffusion confirms this picture for SW Si. From the Arrhenius plot, we obtained an activation energy of 0.54 eV, and a prefactor of 1.3×10^{-3} cm^2/s for the diffusion constant along the dimer rows. The difference between the two measurements of the activation barriers may be the result of the thermal vibrations of the substrate atoms at high temperatures.

The quoted results are in approximate agreement with the results of other molecular-dynamics studies, using different potentials to model the Si.[16,17] The results of all of these studies, however, differ somewhat from those of a recent *ab initio* calculation.[18] While the first-principles calculation predicts faster diffusion along the dimer rows, the predicted path for diffusion is on top of the dimer rows. The anisotropy in the diffusion constants was also found to be larger. Experimental results based on a STM study of island density also point to faster diffusion along dimer rows. The estimated activation energy and prefactor for diffusion are 0.67 ± 0.08 eV and about 10^{-13} cm^2/s, respectively. These results are in excellent (perhaps fortuitous) agreement with those obtained using the SW potential.[17]

We now discuss the potential-energy surface for Ge adatoms on the Si(001) surface. As previously discussed, the Ge atoms were modeled using the empirical Stillinger-Weber potential having both a 4% larger radius and a softer potential. In addition, to disentangle the effects of both of these changes, we repeated the calculations modifying only one of the parameters at a time. Generally speaking, the basic features of the energy surface for Ge on Si(001) are the same as those of Si on Si(001)—only the numerical values of the binding energies and activation energies are somewhat changed.

Consider the case where Ge is modeled as SW Si having both a larger radius and softer potential. We measured binding energies of 2.47 eV for the long-bridge site M_1, 2.06 eV for M_2, 2.09 eV for M_3, and 1.95 eV for M_4. The value of these adsorption energies can easily be understood in terms of the two changes that were made to the potential. Making the pair potential softer decreases the Ge-Si binding. For this case, we measure binding energies of 2.40 eV for M_1, 2.24 eV for M_2, 2.06 eV for M_3, and 1.96 eV for M_4. On the other hand, changing only the adatom radius increases the binding slightly: we measure 3.05 eV for M_1. The binding energy at the other local minima are virtually the same as those for Si on Si(001). This slight increase in the adsorption strength can be understood in terms of the geometry of the binding. Consider a Si adatom sitting at M_1. Here, the dimer bond in the presence of an adatom, as well as the adatom-dimer bond, are under considerable strain, as compared to the dimer bond in the absence of an adatom. Placing a larger atom like Ge at that site will decrease this strain, and, with all other things being equal, lead to a slightly stronger bond.

Figure 5 summarizes the activation energies for diffusion hops of Ge adatoms over the Si(001) surface. Note that, despite differences in the adatom to surface binding, the activation energies for Ge and Si on Si(001) are fairly close. Changing both the radius and the potential increases the anisotropy in the diffusion constants slightly: An activation energy of 0.64 eV is required for a Ge adatom to move down the channel separating the dimer rows, while a barrier of 0.80 eV must be overcome to move across the dimer rows. This slight increase is chiefly due to the change in radius. In the case of a change of radius only, a much larger anisotropy is predicted: The barrier for adatom motion across the dimer rows is now a relatively large 0.99 eV, while the barrier for motion in the channel separating dimer rows is decreased to 0.62 eV. A similar decrease in the activation energy for diffusive motion of Ge on Si(001) was observed in another molecular-dynamics study utilizing a Tersoff potential.[34]

Our results are in agreement with a STM study of Ge diffusion on Si(001),[19] in which estimates for the activation energy of Ge diffusion on Si(001) are given to be 0.59 ± 0.1 eV. While we have not explicitly carried out a

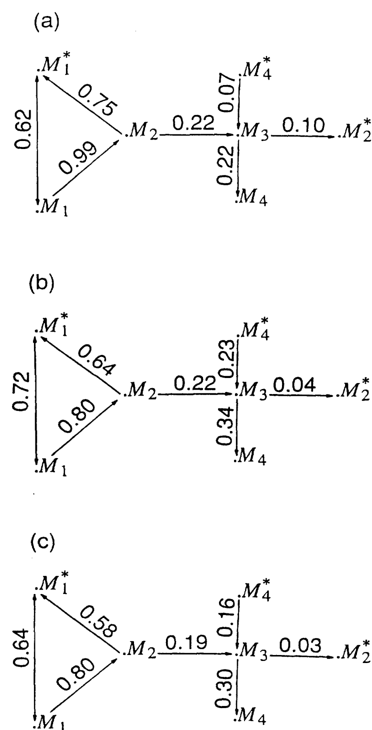

FIG. 5. A summary of the activation energies, given in electron volts (eV), for diffusion hops of Ge adatoms moving over the Si(001) surface. (a) Only the radius of the adatom is made larger. (b) Only the pair potential is made softer. (c) Both the radius and potential are changed.

measurement of the prefactor for Ge diffusion, we do not expect the prefactor to change much. Indeed, the experimental estimate is $\approx 10^{-3}$ cm^2/s, which is very close to our results for Si diffusion on Si(001).[17]

B. Ge diffusion on a Ge_nSi(001) (2×1) surface

We now consider the motion of Ge adatoms over Ge_nSi(001) (2×1) surfaces. We presented detailed results for the Ge_3Si(001) potential-energy surface, which are shown in Fig. 6. (Note that there are no missing dimers, and that the atomic positions are given in Fig. 4.) We do not expect these results to change much for other small values of n.[35] For completeness, we show both the contour plots as well as a summary of the activation energies for the adatom motion. Again, the potential-energy surfaces obtained closely resemble those of a Si adatom over the Si(001) surface.

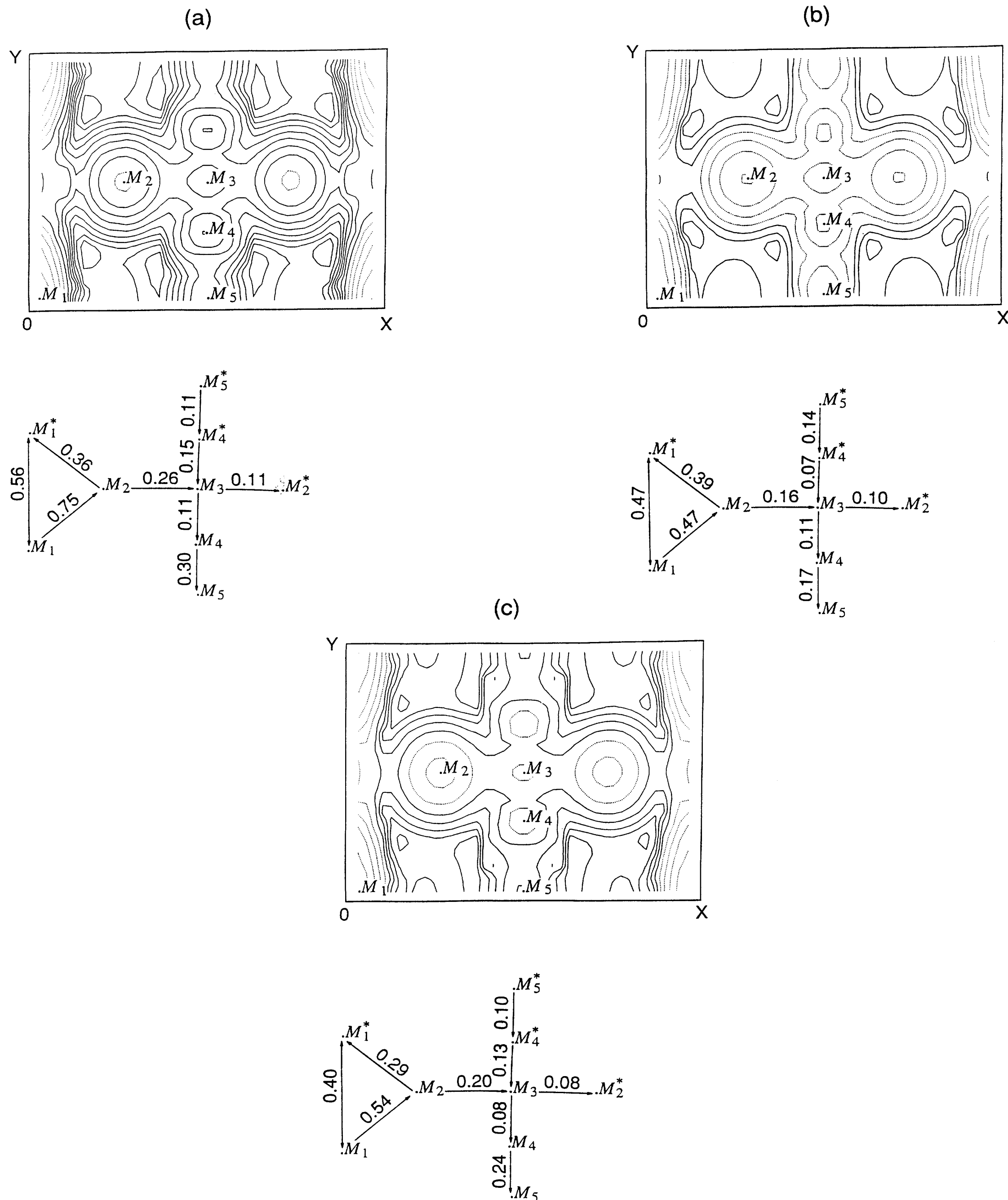

FIG. 6. Contour plots as well as a summary of the activation energies for diffusion hops for a Ge adatom over a Ge_3Si(001) (2×1) surface. (a) Results for Ge modeled as a SW silicon with a larger radius only. (b) Results for Ge modeled with a softer potential only. (c) Results for both a larger radius and softer potential.

The behavior of the Ge adsorption on $Ge_3Si(001)$ (2×1) surface shows similar trends to that of the Ge on the Si(001) surface. The binding sites are all close to the same positions. For Ge modeled as SW silicon, having both a larger radius and softer potential, the binding is 2.34 eV at M_1, 2.08 eV at M_2, 1.96 eV at M_3, 2.00 eV at M_4, and 1.86 eV at M_5, respectively. Again, the softer potential is what gives rise to such a decrease in binding energy. If only the potential is made softer, the binding energies are 2.02 eV for M_1, 1.93 eV for M_2, 1.88 eV for M_3, 1.86 eV for M_4, and 1.83 eV for M_5, respectively. Increasing the radius of only the Ge atoms increases the binding energies slightly. They are 3.25 eV at the long-bridge site M_1, 2.86 eV at M_2, 2.70 eV at M_3, 2.75 eV at M_4, and 2.56 eV at M_5.

Diffusion on the $Ge_nSi(001)$ surface is similar to diffusion on the Si(001) surface. The motion is predicted to be anisotropic, with fast diffusion taking place in the channel separating dimer rows. There are, however, important differences between the case of Ge on $Ge_nSi(001)$ (2×1) and Si on Si(001), the most important one being that the activation energies for hops is considerably less for Ge on $Ge_nSi(001)$ than for Si on Si(001). For example, the activation energy for motion in the channel separating dimers for Si on Si(001) is 0.67 eV; for Ge on $Ge_3Si(001)$, this value has decreased to 0.40 eV. Both the change in the radius and the change in the pair potential account for this result. Relative to a smaller atom, a larger sized atom has a slightly larger interaction range, so that it always "sees more" of the substrate, giving lower activation energy barriers. This lowering of the barriers also means that adatoms will find the minimum-energy positions on the surface. For example, in the case of Si on Si(001), an adatom landing on top of the dimer rows may spend considerable time jumping between M_2 and M_2^* before overcoming the 0.54-eV barrier and finding the long-bridge site M_1. In the case of Ge on $Ge_3Si(001)$, this barrier has decreased to 0.29 eV, so hops from M_2 to M_1 should be relatively easy.

C. Ge diffusion on a $Ge_nSi(001)$ $(2\times N)$ surface

As discussed in Sec. I, Ge layers on top of Si(001) are under strain, some of which may be reduced by introducing a $(2\times N)$ instead of a (2×1) reconstruction. Such a surface consists of rows of dimers, with every Nth dimer missing. The second-layer atoms around the missing dimer move together and form a bond. This rebonding leads to considerable local distortions and tensile stress.

We have mapped out the potential-energy surface of a Ge atom over a $Ge_3Si(001)$ surface, terminated with a (2×10) reconstruction.[36] Figure 7 shows the atomic positions and a contour plot of the potential-energy surface in the vicinity of the missing dimer. Away from the missing dimer, the properties of the $(2\times N)$-reconstructed surface are the same as those of the (2×1)-reconstructed surface, discussed previously. The chief minima around the missing dimer are marked in Fig. 7. M_1 and M_3 correspond to the long-bridge site and the (usual) minima on top of the (2×1) dimers. Note that an "energy channel" has formed directly over the missing dimers. It contains minima M_2, M_3, and M_4. Position M_4 corresponds to the minima M_2 on a (2×1) surface [e.g., see Fig. 6(a)].

The binding at the sites around the missing dimer is stronger than that at corresponding positions on the (2×1) surface. The local tensile stress created by the second-layer rebonding can be offset somewhat by the presence of an adatom. For Ge over $Ge_3Si(001)$ (2×10), we measure a binding energy of 2.83 eV for M_1, M_2, and M_6. The bindings at M_3 and M_5 are 2.37 and 2.54 eV, respectively. The binding about the missing dimer is therefore quite substantial: 2.83 eV is more than 90% of 3.14 eV, the approximate energy of bulk Ge in our model. These numbers are to be contrasted with the bindings if the film atoms have a larger radius only. In that case, the binding energies are 3.14 eV for M_1, 2.94 eV for M_2, 2.51 eV for M_3, 2.71 eV for M_5, and 2.88 for M_6. These energies are stronger than those for Si on Si(001), but still only represent 60–70% of the bulk energy (4.33 eV in this case). The difference is due to extra strain. If the atoms of the film are given a softer potential only (no change in radius), then the binding energies are 2.86 eV for M_1, and 2.38, 3.03, 2.92, and 3.16 eV for M_3, M_2, M_5, and M_6, respectively. For the case of M_6, this represents more than 100% of the bulk value. Clearly, for a film having a softer potential and no lattice mismatch, the $(2\times N)$ reconstruction is not favored.

Figure 8 summarizes the activation energies for the

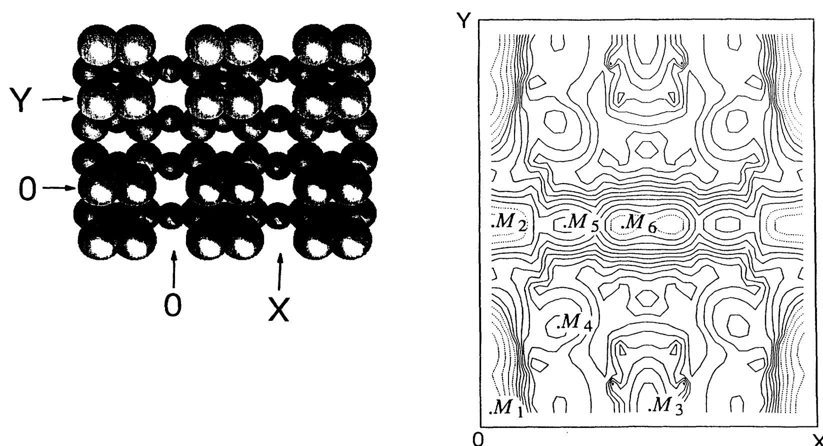

FIG. 7. Contour plots of the potential-energy surface $E(x,y)$ for a Ge adatom (modeled as SW silicon with a larger radius only) over a $Ge_3Si(001)$ (2×10) surface. Also shown are the important atomic positions.

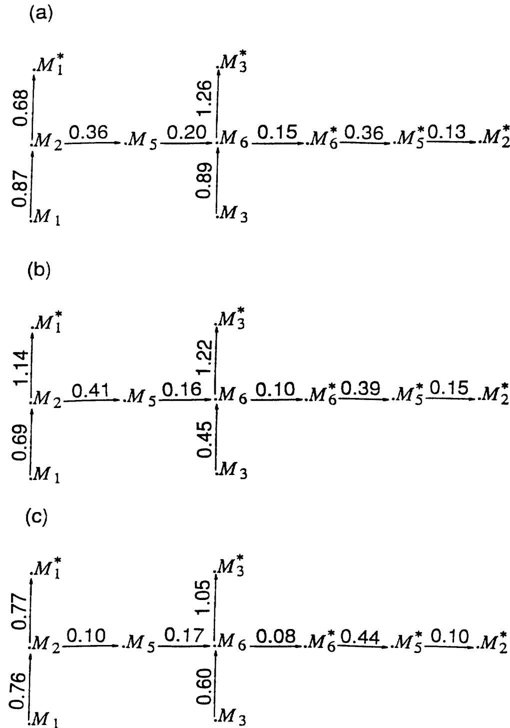

FIG. 8. A summary of the activation energies (in eV) for the most important diffusion hops for Ge over the $Ge_3Si(001)$ (2×10) surface. (a) Results for Ge modeled as having a larger radius only. (b) Results for Ge with a softer potential only. (c) Results for Ge with both a larger radius and softer potential.

significant pathways of the (2×10) surface. Consider an adatom moving along the dimer rows, either in the channel separating the dimers, or on top of them. To reach the missing dimers, the adatom must cross a region of space, where it is relatively "far" away from other atoms. The bonding in this region is therefore reduced, which gives rise to a potential-energy barrier, both to reach the missing dimers, and to leave the channel on top of them. This extra potential barrier is reminiscent of the extra barriers found at the edges of steps, where they may confine the adatoms to a given terrace.[37] Indeed barriers of about 0.76 eV are observed at the missing dimer, and are to be compared to 0.40 eV, which is the activation energy required for motion between long-bridge sites on the (2×1) surface. A schematic of the potential energy along the dimer rows is shown in Fig. 9. On the other hand, the activation energy for diffusion in the channel of the missing dimers is considerably less: only 0.44 eV. In this channel, the adatom can always stay close to the substrate. Films having either a larger radius or a softer potential show similar behavior. Therefore, a single adatom moving over the top of a $Ge_nSi(001)$ surface with $(2\times N)$ reconstructions is expected to move fairly rapidly along the dimer rows, and relatively slowly over the barriers at the missing rows. Since N for the reconstructions varies between 6 and 12, we may therefore expect the adatoms to spend most of their time in the region between the missing rows.

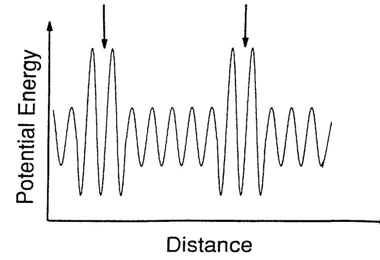

FIG. 9. A schematic of the potential energy vs distance of the $(2\times N)$ surface. The relative large diffusion barriers near the missing dimers are marked with arrows.

To verify the adatom motion, as predicted by the potential-energy surface, we have directly simulated the motion of single adatoms over the $Ge_3Si(001)$ (2×5) surface. Individual adatoms were deposited onto the substrate held at $T=0.9T_M$(Ge), and tracked over a period of about 50 ps. A superposition of the adatom motion, as well as the motion of the first- and second-layer atoms, are shown in Fig. 10. The arrows along the side of the figure mark the location of the missing dimers. The dimer rows run perpendicular to them. As expected, most of the adatom motion conforms to what is predicted by the potential-energy surfaces, and takes place mainly in the channel separating dimer rows. Unlike the case of Si on Si(001), atoms landing on top of the dimer rows soon find the M_1 site, because of the reduced barrier separating M_2 and M_1 sites. Similar to the motion of Si on Si(001),[38] there is evidence for "replacement"-type events. In these situations, the adatom displaces an atom in the surface, with the surface atom becoming the new adatom.

Knowing the values of the activation energies for

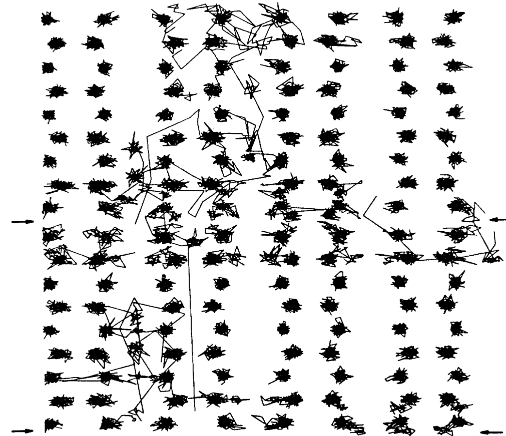

FIG. 10. Trajectories of five different adatoms diffusing over a $Ge_3Si(001)$ (2×5) surface at $T=0.9T_M$, where T_M is the melting temperature of Ge. In this case, Ge is modeled as a SW silicon having both its radius and pair potential changed. Atomic motions of the top two layers are shown. The arrows mark the positions of the missing dimers. Note that most of the adatom motion observed takes place in the channel separating the dimer rows.

diffusion hops, the trends in the diffusion constant may be predicted. The diffusion constant is a measure of the rate of adatom displacement, over large distances and long times. In the direction along the dimer rows, the adatoms move rapidly between the missing dimers, and more slowly over them. Diffusion over large distances will therefore be limited by the largest diffusion barrier, so that we expect the activation energy for diffusion hops along the dimer rows will be close to 0.76 eV, corresponding to the activation energy required to cross the rows of missing dimers. The predominant effect of the minima between the missing rows will be on the prefactor for diffusion: the larger the value of N of the $(2\times N)$ reconstruction, the longer the time spent by the adatom in moving between the missing rows. Similarly, because the activation energy for motion across the dimer rows and between the missing dimers is only 0.54 eV [as opposed to 0.76 eV for Si adatoms moving across dimer rows on Si(001)], the random walk undertaken by a Ge adatom will be less directional in nature. This will further decrease the prefactor for the diffusion constant along the dimer rows.

In contrast, the random walk undergone by an adatom between the missing rows will be almost purely one-dimensional in nature, because there relatively large barriers confine the adatom. Since the activation energy is a low 0.44 eV, motion will be relatively fast, leading to rapid aggregation of adatoms in this channel. However, because adatoms must spend a considerable time finding the minima on top of the dimers, the prefactor for diffusion in this channel can be expected to be considerably reduced.

We believe that this picture of Ge diffusion on Ge_nSi(001) $(2\times N)$ surfaces may explain the recent experimental observations of Lagally and co-workers,[19] who measured an activation energy of 0.45 eV for Ge diffusion, and a prefactor that is $\approx 10^{-6}$ cm^2/s, which is three orders of magnitude less than the prefactor for Si diffusion on Si(100). Their measurement of the diffusion constant is based on a STM study of the number density of islands which form after a certain Ge dosage is deposited. Therefore, their diffusion constant is related to the most rapid mechanism of dimer nucleation. Now consider a small number of Ge atoms deposited on a $(2\times N)$ surface. At low coverages, the number of dimers nucleating will be small. This is because the long-range diffusion needed to bring adatoms together at low coverages is inhibited by the presence of the barrier near the missing rows. Adatoms do eventually overcome these barriers, but then they enter into the channels on top of the missing dimers. Long-range diffusion and therefore nucleation of dimers can then take place in these channels, which may act as heterogeneous nucleation sites. We therefore speculate that the diffusion constant measured by Lagally and co-workers is influenced by mechanism. Note, however, that the activation energy predicted by our model is in excellent agreement with the experimental measurement. Again, while we have not explicitly measured the prefactor for this process, we can expect it to be quite small due to the considerable time taken by adatoms to reach the channel.

IV. GROWTH OF GERMANIUM FILMS

In Sec. I of this paper, we discussed the growth modes of Ge films on Si(001), finding that the system follows the expected Stranski-Krastanov growth mode: three continuous layers form, followed by the growth of three-dimensional islands. The first layer deposited favors a surface with a (2×1) reconstruction, while the second and third layers prefer a $(2\times N)$ reconstruction. The calculation performed was based on equilibrium considerations only, with no reference to the kinetics of growth. To check for possible kinetic pathways, we have carried out extensive molecular-dynamics simulations of Ge growth on the Si(001) surface.

The growth of the initial layer of Ge on Si(001) is very similar to that of Si on Si(001). Growth on a flat (2×1) surface takes place through the nucleation of islands, which grow and eventually coalesce to form a continuous layer. At low coverages and sufficiently high temperatures, highly anisotropic islands or "dimer strings" are formed on the surface. These islands have been observed in STM work on Ge on Ge(001).[3] The origin of the elongated shape of these islands lies in the differing growth properties of the Si(001) steps. The long side of the islands resembles the S_A steps, which, at low coverages, are characterized by a slow rate of advance.[39] However, there is relatively "fast" diffusion along the long side of the dimer strings, so that material gets preferentially transported toward the ends of the dimer rows where enhanced growth takes place. We simulated the

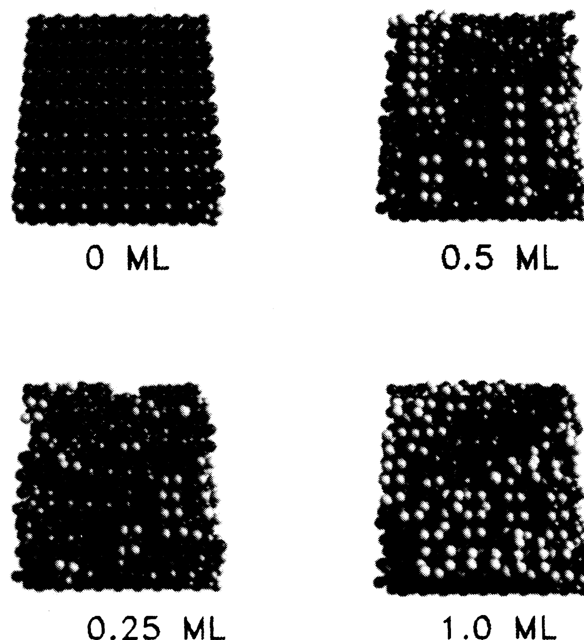

FIG. 11. Configurations of the structures obtained as one monolayer (ML) of Ge atom is deposited onto a Si(001) substrate. Growth parameters are given in the text. Note the formation of dimer strings. Atoms are shaded according to height, with the higher atoms having a lighter shade.

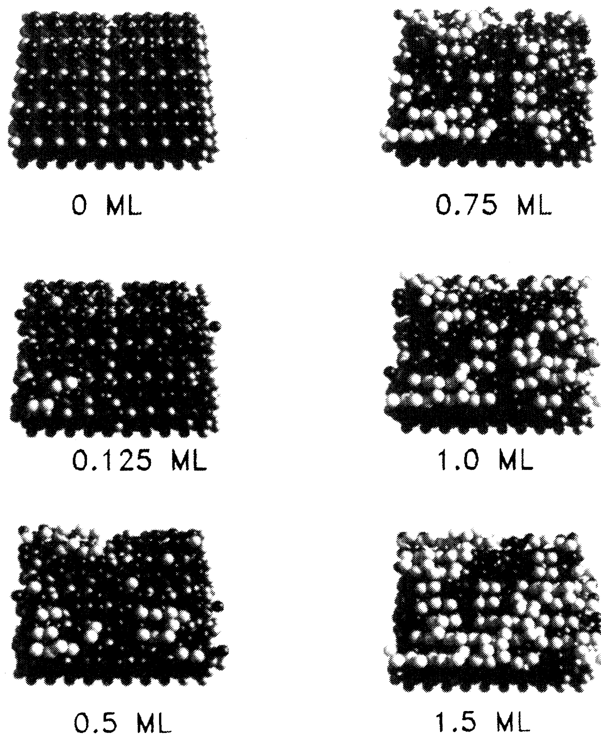

FIG. 12. Atomic configurations as obtained by a molecular-dynamics simulation of Ge on $Ge_3Si(001)$ (2×5) surface. The rate of deposition was one monolayer in 0.24 ns; substrate temperature was held at $T=0.9T_M$ (Ge).

growth of the first Ge layer on Si(001). Ge atoms, modeled as discussed in Sec I, were deposited onto a six-layer 12×10 Si(001) substrate held at a temperature of about 1130 K. The rate of deposition was about one monolayer (ML) per ns. While this rate of deposition is eight to ten orders of magnitude larger than laboratory deposition rates, we still observe the formation of dimer strings, and their eventual coalescence.[40] Configurations are shown in Fig. 11.

Growth of the second monolayer on Si(001) will be similar, except that now the surface tends to form the $(2\times N)$ "missing dimer" reconstruction. We have simulated the growth of Ge on a $Ge_3Si(001)$ (2×5) surface, which is where three-dimensional islanding may first be expected. Deposition of Ge was carried out at a rate of one monolayer per 0.24 ns, onto a six-layer 8×10 substrate at 1130 K. During the simulation, the bottom two layers were kept static. Configurations are shown in Fig. 12. While the deposit does seem to be rougher than the corresponding one for Ge on Si(001) (Fig. 10), it is difficult to know whether the initial stages of three-dimensional islanding are seen, both because of the strong finite-size effects and the high deposition rates. Figure 13 offers a more direct comparison. It shows configurations at coverages of 0.5 and 1.0 monolayers of Si on Si(001) (2×5) (this reconstruction was used in order to make a fair comparison), and Ge on $Ge_3Si(001)$ and $Ge_6Si(001)$. The simulation parameters were the same as for Fig. 12. The enhanced roughness is now quite visible. Indeed, it seems that on the six-layer film, where the driving force for clustering is much stronger than on the three-layer film, a three-dimensional island is beginning to form.

V. SUMMARY

In summary, we have studied the growth of Ge layers on Si(001). In agreement with experiments and other calculations, the model predicts that the growth will follow a Stranski-Krastanov mode, with three continuous layers forming initially. In contrast to Si on Si(001), the upper surface will be terminated with a $(2\times N)$ reconstruction. These features are due to the strain in the films, which results from the mismatch between the Si and Ge atoms.

Diffusion of Ge adatoms on the $Ge_nSi(001)$ (2×1) surface will be similar to that of Si on Si(001). Fast diffusion is predicted to take place along the dimer rows. However, the activation energies for Ge diffusion are lower than those for Si, so that the overall diffusion of Ge is expected to be faster. In the case of surfaces terminated with a

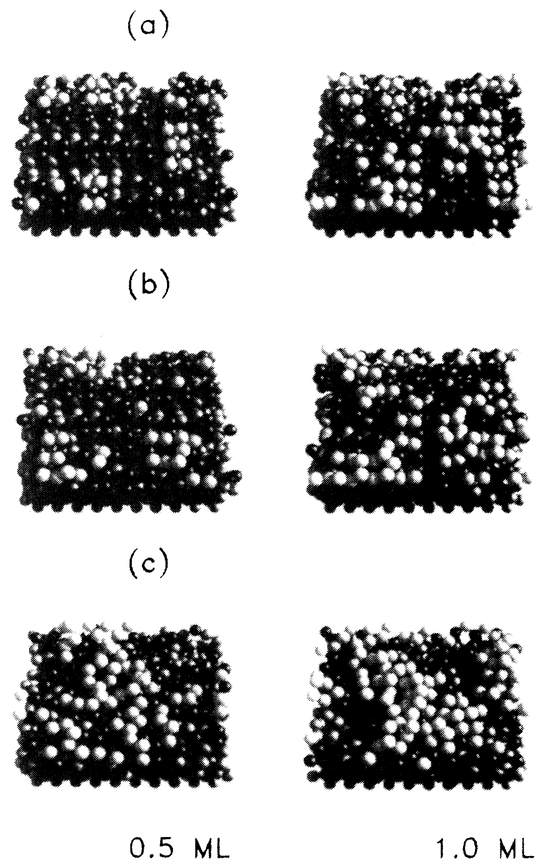

FIG. 13. A comparison of various thin-film structures obtained when (a) silicon was deposited on a Si(001) (2×5) surface; (b) Ge was deposited on a $Ge_3Si(001)$ (2×5) surface; and (c) Ge was deposited on a $Ge_6Si(001)$ (2×5) surface. The rate of deposition in all cases was one monolayer in 0.24 ns. Throughout the simulation, the substrate temperature was held at $T=0.9T_M$ (Ge).

$(2\times N)$ missing dimer reconstruction, the presence of additional diffusion barriers is observed on both sides of the rows of missing dimers. The channel on top of the missing dimers therefore acts as a heterogeneous nucleation site for dimers, acting in many ways like a step edge. Finally, we have studied the growth of Ge layers by molecular-dynamics deposition experiments. Similar to the case of Si on Si(001), we have observed the formation and growth of dimer strings of Ge on Si(001). Deposits formed on three- and six-layer films show some evidence of clustering.

In conclusion, we emphasize that our calculations were based on potentials which do not provide a perfect description of real semiconductor surfaces. However, the effects of strain fields at the atomic level are treated correctly, and our results are in good agreement with experimental work and the results of other models. We believe that molecular-dynamics studies will continue to provide insight into the growth properties of real materials.

ACKNOWLEDGMENTS

We would like to thank Dr. David Eaglesam and Dr. Marcia Grabow for useful discussions and a critical reading of the manuscript. One of us (C.R.) would like to thank the Natural Sciences and Engineering Research Council of Canada for financial support.

[1]J. A. Morianty and S. Krishnamurthy, J. Appl. Phys. **54**, 1892 (1983); R. People, J. C. Bean, D. V. Lang, A. M. Segent, H. L. Stoermer, K. W. Wecht, R. T. Lynch, and K. Baldwin, Appl. Phys. Lett. **45**, 1231 (1984); T. P. Pearsall, H. Temkin, J. C. Bean, and S. Luryi, IEEE Electron Device Lett. **7**, 1330 (1986); T. P. Pearsall, J. Bevk, L. C. Feldman, J. M. Bonar, J. P. Mannarts, and A. Ourmazd, Phys. Rev. Lett. **58**, 729 (1987).

[2]A variety of techniques have been used to study this system. See, for example, B.-Y. Tsaur, M. W. Geis, J. C. Fan, and R. P. Gale, Appl. Phys. Lett. **38**, 779 (1981); M. Asai, H. Ueba, and C. Tatsujama, J. Appl. Phys. **58**, 2577 (1985); K. Sakamoto, T. Sakamoto, S. Nagao, G. Hashiguchi, K. Kuriyoshi, and Y. Bondo, Jpn. J. Appl. Phys. **26**, 666 (1987); Y. Koide, S. Zaima, N. Oshima, and Y. Yasuda, *ibid.* **28**, 690 (1989); P. M. Maree, K. Nakajama, F. M. Mulders, and J. F. van der Veen, Surf. Sci. **191**, 305 (1987).

[3]A good review is J. E. Griffith and G. P. Kochanski, CRC Crit. Rev. Solid State Mater. Sci. **16**, 305 (1990).

[4]A. Ourmazd and J. C. Bean, Phys. Rev. Lett. **55**, 765 (1985).

[5]P. C. Kelieres and J. Tersoff, Phys. Rev. Lett. **55**, 765 (1985).

[6]F. K. LeGoues, V. P. Kesan, S. S. Iyer, J. Tersoff, and R. Tromp, Phys. Rev. Lett. **64**, 2038 (1990).

[7]D. E. Jesson, S. J. Pennycook, and J. M. Baribeau, Phys. Rev. Lett. **66**, 750 (1991); D. E. Jesson, S. J. Pennycook, J. M. Baribeau, and D. C. Houghten, *ibid.* **64**, 2062 (1992).

[8]D. J. Eaglesham and M. Cerullo, Phys. Rev. Lett. **64**, 1943 (1990).

[9]Y.-W. Mo, D. E. Savage, B. S. Schwartzentruber, and M. G. Lagally, Phys. Rev. Lett. **65**, 1020 (1990).

[10]Y.-W. Mo and M. G. Lagally, J. Cryst. Growth **111**, 876 (1991).

[11]F. K. LeGoues, M. Copel, and R. M. Tromp, Phys. Rev. B **42**, 11 690 (1990).

[12]M. Asai, H. Veber, and C. Tatsuyama, J. Appl. Phys. **58**, 2577 (1985); H. J. Gossman, L. C. Feldman, and W. M. Gibson, Surf. Sci. **155**, 413 (1985).

[13]J. Tersoff, Phys. Rev. B **43**, 9377 (1991).

[14]J. Tersoff, Phys. Rev. B **45**, 833 (1992).

[15]Y.-W. Mo and M. G. Lagally, Surf. Sci. **248**, 313 (1991); Y.-W. Mo, J. Kleiner, M. B. Webb, and M. G. Lagally, Phys. Rev. Lett. **66**, 1998 (1991).

[16]Molecular-dynamics studies of Si diffusion on Si(001) have been performed by J. Wang and A. Rockett, Phys. Rev. B **43**, 12 571 (1991); D. W. Brenner and B. J. Garrison, Surf. Sci. **198**, 151 (1988); Z. Zhang, Y. Lu, and H. Metiu, Surf. Sci. Lett. **248**, L50 (1991).

[17]C. Roland and G. H. Gilmer, Phys. Rev. B **46**, 13 428 (1992).

[18]G. Brocks, D. J. Kelly, and R. Car, Phys. Rev. Lett. **66**, 1729 (1991); T. Miyazuki, H. Hiromoto, and M. Okazoki, Jpn. J. Appl. Phys. **29**, L1165 (1990).

[19]D. Raitt, J. Rownd, F. Wu, and M. G. Lagally (unpublished); M. G. Lagally (private communication).

[20]For example, see references cited in Ref. 3.

[21]F. C. Frank and J. H. van der Merwe, Proc. R. Soc. London Ser. A **198**, 205 (1949).

[22]M. Volmer and A. Weber, Z. Phys. Chem. **119**, 277 (1926).

[23]I. N. Stranski and V. L. Krastanov, Akad. Wiss. Lit. Mainz Math. Naturwiss K1. Karl-August-Forster Lec. **146**, 797 (1939).

[24]D. A. Huse, Phys. Rev. B **29**, 6985 (1984).

[25]R. Bruinsma and A. Zangwill, Europhys. Lett. **4**, 729 (1987).

[26]M. H. Grabow and G. H. Gilmer, Surf. Sci. **194**, 333 (1988).

[27]K. C. Pandey, in *Proceedings of the Seventeenth International Conference on the Physics of Semiconductors,* edited by J. D. Chadi and W. A. Harrison (Springer-Verlag, New York, 1985).

[28]For a general reference, see R. W. Hockney and J. W. Eastwood, *Computer Simulations Using Particles* (McGraw-Hill, New York, 1981).

[29]F. H. Stillinger and T. A. Weber, Phys. Rev. B **31**, 5262 (1985).

[30]The dimers predicted by the SW model are symmetric, rather than asymmetric. However, because the energies involved are rather small, this will not have much of an effect on the potential-energy surface. Furthermore, what we really wish to understand is the diffusion at room temperature or above, where the dimers appear symmetric because of thermal motion.

[31]As a first approximation, we shall consider relaxed film structures, where the Ge sits on the Si(001) substrate only. Therefore we neglect possible mixing and alloying effects, which may be important if true equilibrium between the film and substrate is to be established. This should be a reasonable approximation, providing that bulk diffusion is negligible.

[32]We have not tried to find the optimum values of N, for the Ge_nSi(001) $(2\times N)$ structures. Tersoff (Ref. 14) shows that $N\approx 8$ is the preferred reconstruction for a Keating model.

[33]We expect the Ge(001) steps to be very similar to the Si(001) steps. See J. Chadi, Phys. Rev. Lett. **59**, 1691 (1987).

[34]Diffusion of Ge on Si(001) was also studied using a Tersoff potential by D. Srivastava and B. J. Garrison, Phys. Rev. B **46**, 1472 (1992). In this study, diffusion of Ge is predicted to be slightly slower than that of Si. This decrease seems to be due to a decrease in their predicted prefactor, which was calculated using a Voter model.

[35]We checked a small number of paths at $n=1$, 2, and 4, finding virtually identical results to those at $n=3$.

[36]We do not expect the potential-energy surface of other $(2\times N)$ surfaces to differ much.

[37]Barriers at step edges can give rise to growth instabilities: R. L. Schwoebel, J. Appl. Phys. **37**, 3682 (1966); G. H. Gilmer, R. Ghez, and N. Cabrera, J. Cryst. Growth **8**, 79 (1971).

[38]G. H. Gilmer and C. Roland (unpublished).

[39]C. Roland and G. H. Gilmer, Phys. Rev. Lett. **67**, 3188 (1991); Phys. Rev. B **46**, 13 437 (1992).

[40]In molecular-dynamics simulations, large deposition rates are required because of the finite computer time available.

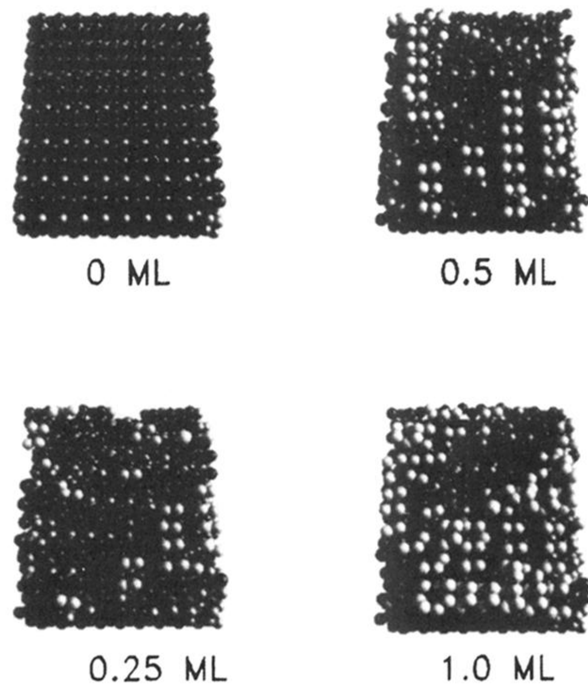

FIG. 11. Configurations of the structures obtained as one monolayer (ML) of Ge atom is deposited onto a Si(001) substrate. Growth parameters are given in the text. Note the formation of dimer strings. Atoms are shaded according to height, with the higher atoms having a lighter shade.

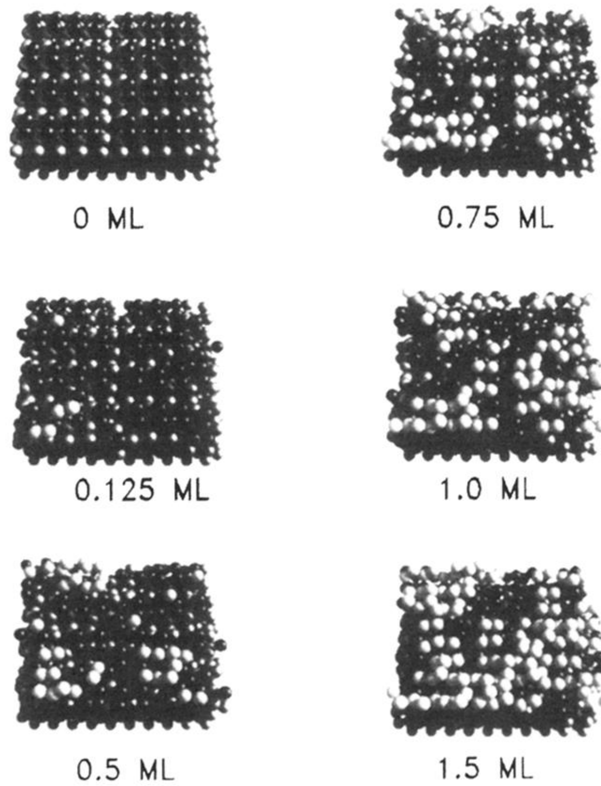

FIG. 12. Atomic configurations as obtained by a molecular-dynamics simulation of Ge on $Ge_3Si(001)$ (2×5) surface. The rate of deposition was one monolayer in 0.24 ns; substrate temperature was held at $T=0.9T_M$ (Ge).

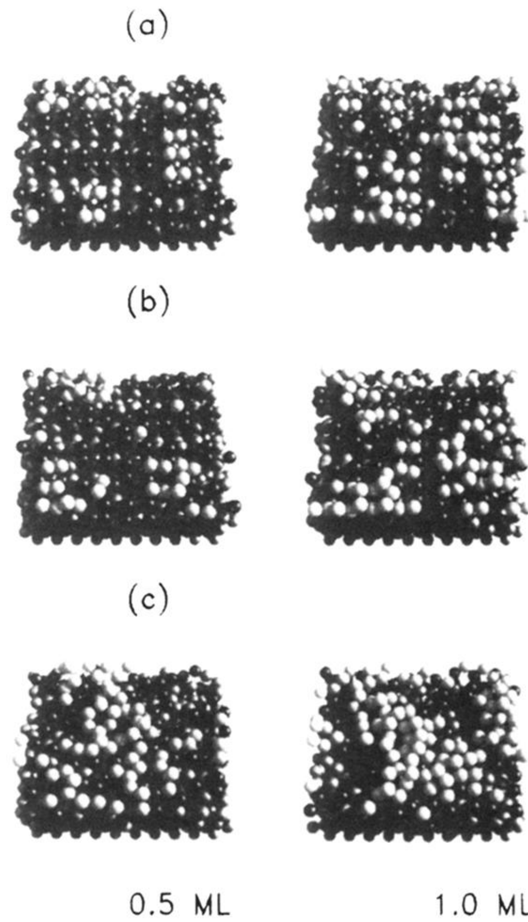

FIG. 13. A comparison of various thin-film structures obtained when (a) silicon was deposited on a Si(001) (2×5) surface; (b) Ge was deposited on a $Ge_3Si(001)$ (2×5) surface; and (c) Ge was deposited on a $Ge_6Si(001)$ (2×5) surface. The rate of deposition in all cases was one monolayer in 0.24 ns. Throughout the simulation, the substrate temperature was held at $T=0.9T_M$ (Ge).